Journal of Vertebrate Paleontology 30(5):1579–1593, September 2010

ARTICLE

A LARGE-BODIED ANOMALUROID RODENT FROM THE EARLIEST LATE EOCENE OF EGYPT: PHYLOGENETIC AND BIOGEOGRAPHIC IMPLICATIONS

HESHAM M. SALLAM,*[,1] ERIK R. SEIFFERT,[2] ELWYN L. SIMONS,[3] and CHLÖE BRINDLEY[1]
[1]Department of Earth Sciences, University of Oxford, Parks Road, Oxford, OX1 3PR, United Kingdom, sallam@mans.edu.eg; chloe.brindley@gmail.com;
[2]Department of Anatomical Sciences, Stony Brook University, Stony Brook, New York 11794-8081, U.S.A., erik.seiffert@stonybrook.edu;
[3]Division of Fossil Primates, Duke Lemur Center, 1013 Broad Street, Durham, North Carolina 27705, U.S.A., esimons@duke.edu

ABSTRACT—A new genus and species of anomaluroid rodent, *Kabirmys qarunensis*, is described based on isolated teeth, partial mandibles, and an edentulous partial maxilla from the earliest late Eocene Birket Qarun Locality 2 (BQ-2) in the Fayum Depression of northern Egypt. *Kabirmys* is the largest known Paleogene anomaluroid, with first lower molar area being about 2.5 times that of the roughly contemporaneous *Nementchamys* and *Pondaungimys* from Algeria and Myanmar, respectively. The genus exhibits distinctive features not seen in other Paleogene taxa, such as a complete mure, weak neo-endoloph, and open lingual sinus on the upper molars; *Kabirmys* lacks the complex enamel crenulations seen in *Nementchamys* and *Pondaungimys*. Phylogenetic analysis of dental features nests *Kabirmys* within crown Anomaluridae as a sister taxon of *Nementchamys* and *Pondaungimys*, but parsimony analysis following addition of a chronobiogeographic character places all of these taxa as basal stem members of Anomaluridae. This new evidence indicates that there was considerable diversity in body size and molar morphology among African anomaluroids near the middle-late Eocene boundary, and suggests that the group had an ancient origin on that landmass. *Kabirmys* shares some primitive features with the possible zegdoumyid '*Glibia*' *namibiensis* from the Paleogene of Namibia, and suggests that anomaluroids might be derived from a zegdoumyid-like ancestor. The disappearance of anomaluroids in the upper (latest Eocene to early Oligocene) levels of the Fayum succession might be related to global cooling through the later Paleogene, which might have removed suitable habitats from northern Africa.

INTRODUCTION

The rodent family Anomaluridae, commonly known as the 'scaly-tailed flying squirrels,' is represented by three living genera (*Anomalurus*, *Idiurus*, and *Zenkerella*) that are restricted to forests of equatorial Africa (Kingdon, 1997). In the later Eocene, anomaluroids ranged into northern Africa and even southeast Asia (Jaeger et al., 1985; Dawson et al., 2003; Marivaux et al., 2005). The first definitive appearance of Anomaluroidea in the fossil record derives from three roughly contemporaneous localities near the middle-late Eocene boundary: *Nementchamys* (Jaeger et al., 1985) and *Shazurus* (Sallam et al., 2010) have been recovered from the late Eocene of Algeria and Egypt, respectively, whereas *Pondaungimys* is known from the latest middle Eocene of Myanmar (Dawson et al., 2003; Marivaux et al., 2005). The latter is the only undoubted occurrence of an anomaluroid outside of Afro-Arabia. Anomaluroids have never been recovered from the well-sampled latest Eocene and Oligocene Fayum localities in northern Egypt (Fig. 1), but have been reported (though not illustrated) from the Oligocene of Oman (Thomas et al., 1999). The clade is represented in the Miocene of east Africa by species placed in the genera *Paranomalurus* and *Zenkerella* (Lavocat, 1973; Winkler, 1992). Recent molecular phylogenetic analyses of the Order Rodentia have placed Anomaluridae as the sister group of the endemic African family Pedetidae (spring hares) within the superfamily Anomaluroidea (Huchon et al., 2007), and the group as a whole may be derived from the early or early middle Eocene rodent family Zegdoumyidae (Vianey-Liaud and Jaeger, 1996), at present known from Algeria (Vianey-Liaud et al., 1994) and Namibia (Pickford et al., 2008).

The diminutive and highly derived anomalurid *Shazurus* has recently been reported from Birket Qarun Locality 2 (BQ-2), which occurs in the Umm Rigl Member of the Birket Qarun Formation, in the Fayum Depression of northern Egypt (Fig. 2) (Sallam et al., 2010). Evidence from magnetostratigraphy (Seiffert et al., 2005, 2008; Seiffert, 2006), sequence stratigraphy, and invertebrate biostratigraphy (Gingerich, 1992) supports an earliest late Eocene (earliest Priabonian, ~37 Ma) age for the locality (Seiffert et al., 2008). Here we describe the upper and lower dentition and maxillary and mandibular morphology of a new, much larger, genus and species of anomaluroid, one of the more common mammals at Locality BQ-2. The locality has also produced remains of primates (Seiffert et al., 2003, 2005, 2009), hystricognathous rodents (Sallam et al., 2009), bats (Gunnell et al., 2008), macroscelideans, and tenrecoids, as well as larger mammals such as proboscideans (Liu et al., 2008), hyracoids (Barrow et al., 2010), hyaenodontid creodonts, and ptolemaiids (Cote et al., 2007). Deposits that are situated stratigraphically above and below Locality BQ-2 are nearshore marine in origin, but the terrestrial mammal-bearing lenses at BQ-2 and nearby localities represent freshwater fluvial beds that were evidently laid down during a sea-level lowstand (Seiffert et al., 2008).

Dental terminology follows Marivaux et al. (2005) (Fig. 3).

Institutional Abbreviations—**CGM**, Egyptian Geological Museum, Cairo; **DPC**, Duke Lemur Center, Division of Fossil Primates.

*Corresponding author.

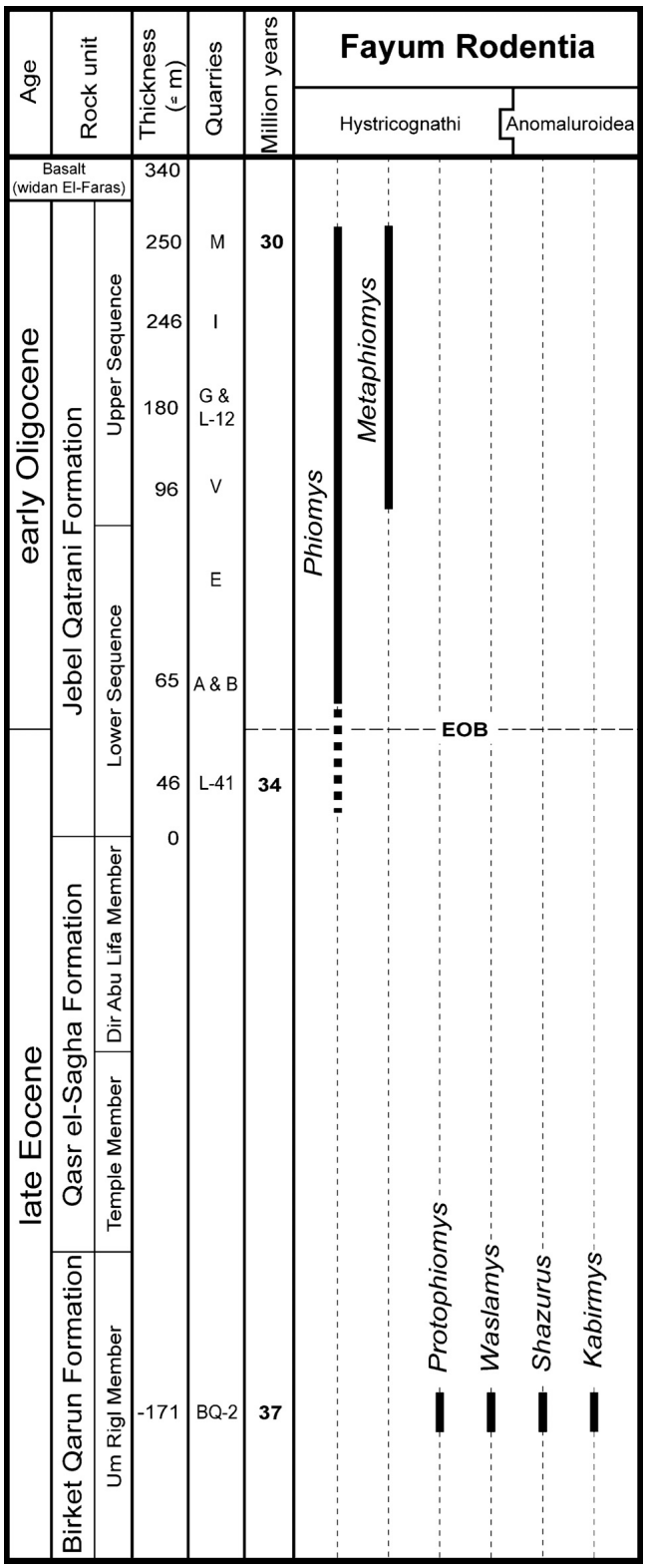

FIGURE 1. Stratigraphic ranges of described Fayum phiomorph and anomaluroid rodents. Age estimates for major mammal-bearing fossil localities, and approximate position of Eocene-Oligocene boundary, follows Seiffert (2006).

SYSTEMATIC PALEONTOLOGY

Class MAMMALIA Linnaeus, 1758
Order RODENTIA Bowdich, 1821
Superfamily ANOMALUROIDEA Gervais, 1849
Family ANOMALURIDAE Gill, 187
Genus *KABIRMYS*, gen. nov.

Type Species—*Kabirmys qarunensis*, sp. nov.

Etymology—Combination of *kabir* (pronounced kuh-BEER), Arabic for 'big,' in reference to the large size of this genus, and *mys*, Greek for mouse.

Generic Diagnosis—As for the type species.

Range—Birket Qarun Formation, Umm Rigl Member (earliest late Eocene).

KABIRMYS QARUNENSIS, sp. nov.
(Figs. 4, 6, 7, 8, Table 1)

Etymology—For the nearby lake Birket Qarun.

TABLE 1. Measurements for upper and lower teeth of *Kabirmys qarunensis*, gen. et sp. nov.

Specimen No.	Tooth		Length (mm)	Width (mm)
Lower teeth				
DPC 21374A	Left	dp4	3.35	2.40
DPC 21452B	Left	dp4	3.50	2.45
DPC 21221B	Left	dp4	3.50	2.65
DPC 21360A	Left	dp4	3.70	2.70
DPC 21839A	Left	dp4	3.90	2.80
DPC 23305C	Left	dp4	3.30	2.35
DPC 21294B	Right	dp4	3.80	2.80
DPC 21538B	Right	dp4	3.45	2.55
DPC 21293M	Right	dp4	3.35	2.35
DPC 21358B	Right	dp4	3.65	2.50
DPC 21296E	Left	dp4	3.60	2.70
CGM 08–289A	Left	dp4	3.60	2.50
DPC 21500K	Right	p4	3.50	2.85
DPC 22442H	Left	p4	3.75	3.25
DPC 21839B	Left	p4	3.80	3.25
DPC 23305D	Right	p4	3.95	3.10
DPC 21538C	Left	m1	3.65	3.05
DPC 21221C	Left	m1	3.80	3.30
DPC 21294C	Left	m1	3.75	3.20
DPC 21839G	Left	m1	4.00	3.40
DPC 21358C	Right	m1	3.90	3.20
DPC 21360B	Right	m1	3.85	3.15
DPC 23305F	Right	m1	4.00	3.40
CGM 83698	Right	m1	3.80	3.30
CGM 83698	Right	m2	3.80	3.40
DPC 21374B	Right	m2	3.95	3.55
DPC 21452C	Right	m2	3.50	3.15
DPC 21500L	Right	m2	3.65	3.30
DPC 21538D	Right	m2	3.45	3.15
DPC 21839C	Right	m2	3.65	3.25
DPC 22442I	Right	m2	3.75	3.25
DPC 21360C	Right	m2	3.65	3.15
DPC 21221D	Right	m2	3.75	3.20
DPC 21294D	Left	m2	3.50	3.25
DPC 21296G	Left	m2	3.60	3.25
DPC 21306D	Left	m1 or m2	4.00	3.45
DPC 21374C	Right	m3	3.65	3.10
DPC 23305E	Right	m3	3.60	3.15
DPC 21452D	Left	m3	3.50	2.95
DPC 21358D	Left	m3	3.70	2.95
DPC 21502A	Right	dp4	3.85	2.70
DPC 21747H	Right	dp4	3.55	2.60
DPC 21220C	Right	m2	3.85	3.25
DPC 21488C	Right	m1	4.10	3.40
DPC 21371H	Right	m2	3.60	3.30
DPC 21839D	Right	m1	3.75	3.45

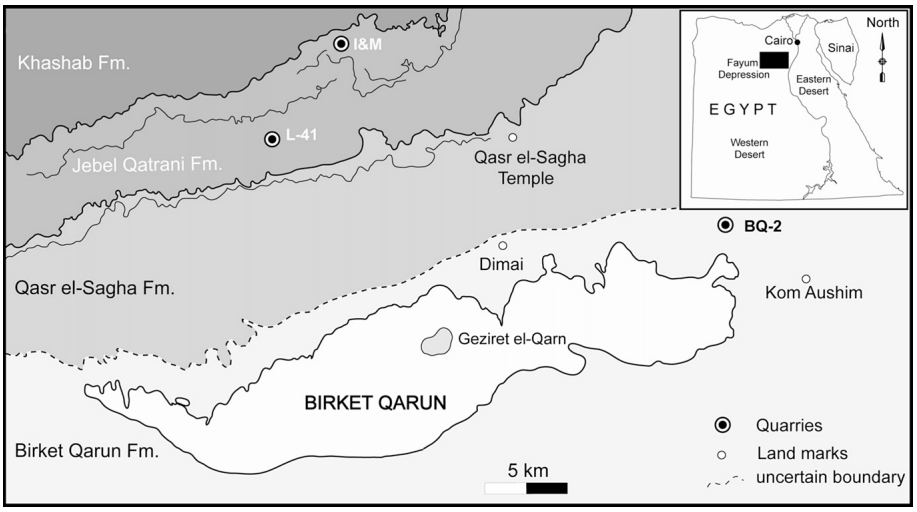

FIGURE 2. Map of the Fayum Depression, northern Egypt. Locality BQ-2 occurs near the northeastern end of Birket Qarun, and to the northwest of Kom Aushim. The boundary between the Umm Rigl Member of the Birket Qarun Formation and the Temple Member of the Qasr el-Sagha Formation is poorly defined and marked here by a dotted line.

TABLE 1. Measurements for upper and lower teeth of *Kabirmys qarunensis*, gen. et sp. nov. *(Continued)*

Specimen No.	Tooth		Length (mm)	Width (mm)
Upper teeth				
DPC 21839E	Left	DP4	3.40	3.40
DPC 21538E	Left	DP4	3.10	3.10
DPC 21502B	Left	DP4	3.10	3.25
DPC 21220D	Right	DP4	3.20	3.10
DPC 21360E	Right	DP4	3.15	3.00
CGM 08–328A	Right	DP4	3.39	3.51
DPC 21294E	Right	P4	3.80	3.80
DPC 21371I	Left	P4	3.75	3.85
DPC 21488D	Left	P4	3.50	3.65
DPC 22442J	Right	M	3.45	3.50
DPC 21347D	Right	M	3.50	3.55
DPC 21747I	Right	M	3.50	3.75
DPC 21452E	Right	M	3.20	3.25
DPC 21220E	Right	M	3.20	3.60
DPC 21358E	Right	M	3.30	3.50
DPC 21488E	Right	M	3.55	3.65
DPC 21374E	Left	M	3.60	3.75
DPC 21371J	Left	M	3.35	3.85
DPC 21293N	Left	M	3.30	3.55
DPC 21294F	Left	M	3.45	3.60
DPC 21358H	Left	M	3.50	3.85
DPC 21360F	Left	M	3.55	3.75
DPC 21488F	Left	M	3.50	3.65
DPC 21839F	Left	M	3.35	3.45
DPC 23305F	Left	M	3.30	3.65
DPC 21502C	Left	M	3.75	3.85
DPC 21538F	Left	M	3.30	3.80
DPC 21221E	Left	M	3.25	3.50
DPC 21296H	Left	M	3.15	3.65
DPC 21452F	Left	M	3.00	3.45
DPC 21500M	Left	M	3.50	3.70
DPC 21220F	Right	M3	3.45	3.35
CGM 08–328B	Left	M3	3.45	3.04
DPC 21221F	Right	M3	2.80	3.00
DPC 21293O	Right	M3	3.20	3.35
DPC 21358G	Left	M3	3.30	3.50
DPC 21488G	Left	M3	3.40	3.30
DPC 21452G	Left	M3	3.25	3.30
DPC 21374F	Left	M	3.65	4.00
DPC 21371K	Right	M	3.30	3.60
DPC 21747J	Right	M	3.20	3.60

Holotype—CGM 83698, right mandible with m1–2 (Fig. 8C, D).

Paratypes—The hypodigm for *Kabirmys qarunensis* includes 70 isolated teeth, one maxillary fragment, and three mandibular fragments: DPC 24494, fragment of left maxilla with P^4 and M^1 alveoli; CGM 08-289A, fragment of left mandible with dp4 and incisor; CGM 21839G, left mandibular fragment with m1; DPC

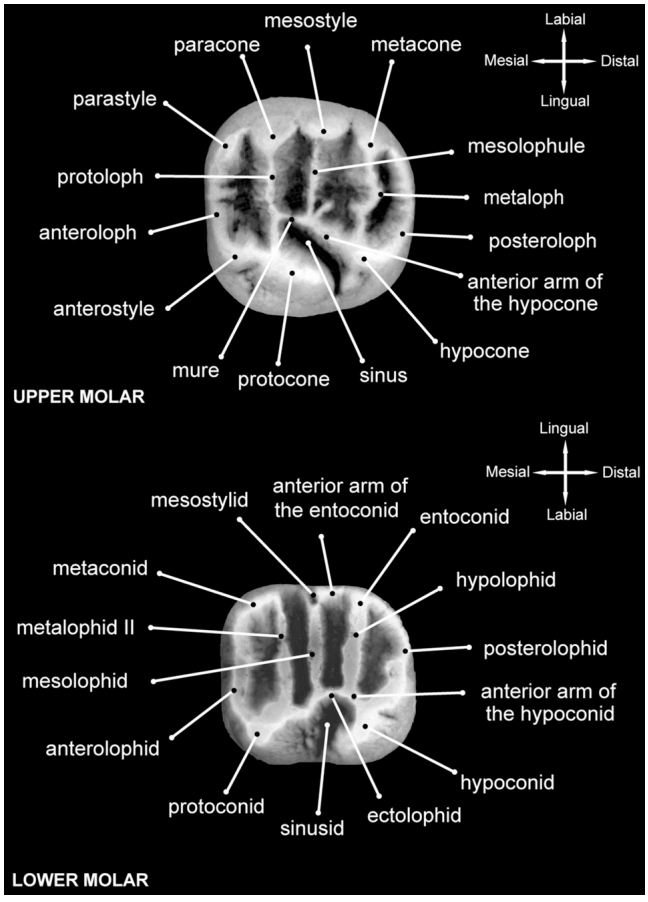

FIGURE 3. Dental terminology, following Marivaux et al. (2005).

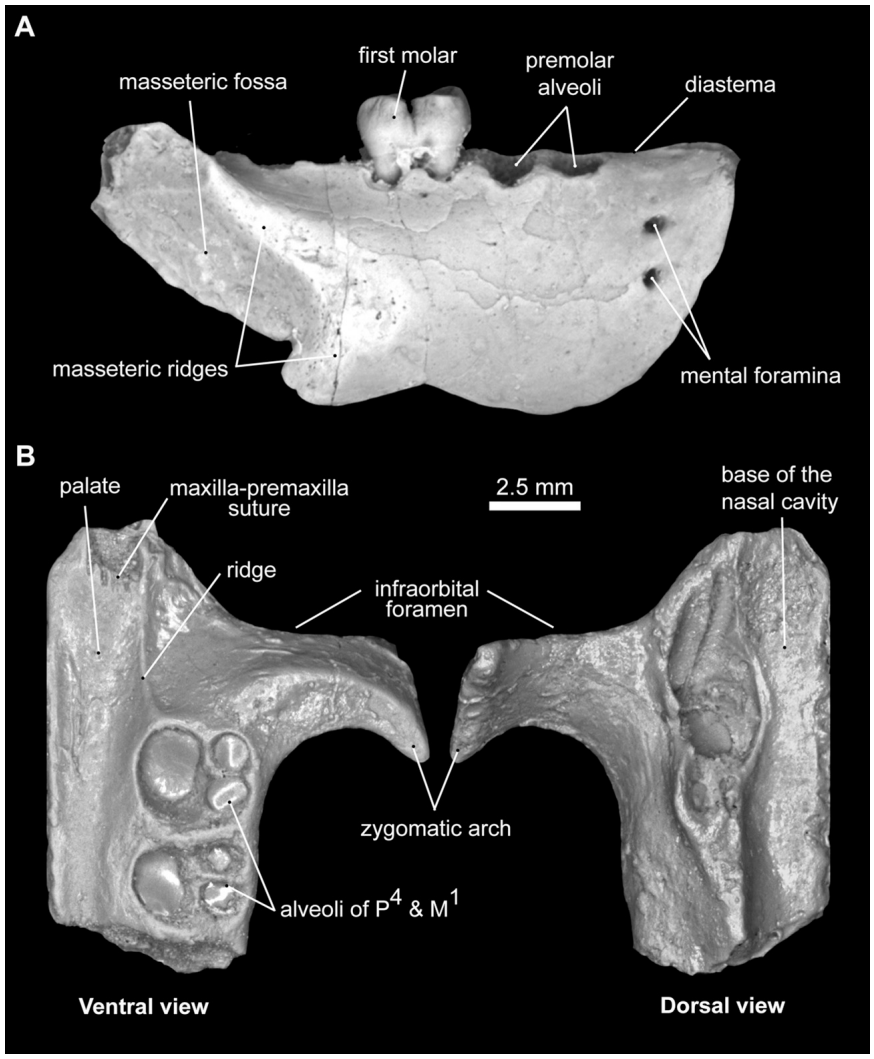

FIGURE 4. **A**, DPC 23305I, right mandible of *Kabirmys qarunensis*, gen. et sp. nov., with m1 and alveoli for p4, m2, and m3, showing morphology of mandibular corpus and masseteric fossa, and position of mental foramina; **B**, cast of DPC 24494, left partial maxilla of *Kabirmys qarunensis*, with alveoli for P^3 and M^1, in ventral and dorsal views.

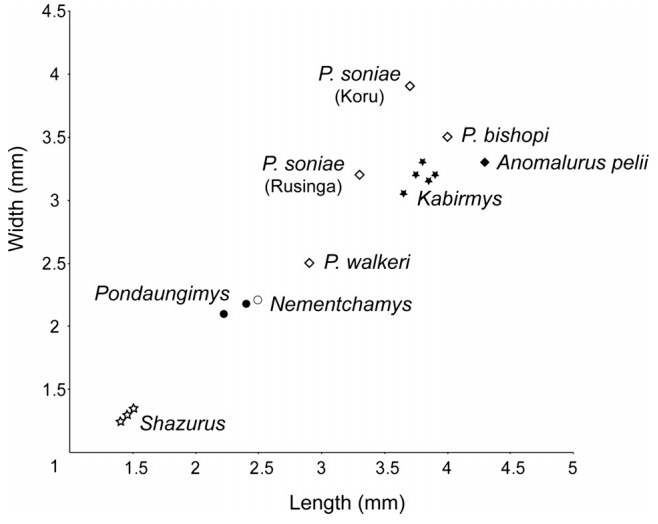

FIGURE 5. Plot of length versus width of m1 for various fossil and extant anomaluroids. Measurements for *Paranomalurus* are from Lavocat (1973). **Symbols**: *Shazurus*, open stars; *Kabirmys*, closed stars; *Nementchamys*, open circle; *Pondaungimys*, closed circles; *Paranomalurus*, open diamonds; *Anomalurus*, closed diamond.

23305I, right mandible with m1 and alveoli for p4, m2, and m3; DPC 23305F, left M1 or M2; DPC 21374A, left dp4; DPC 21452B, left dp4; DPC 21221B, left dp4; DPC 21360A, left dp4; DPC 21839A, left dp4; DPC 23305C, left dp4; DPC 21294B, right dp4; DPC 21538B, right dp4; DPC 21293M, right dp4; DPC 21358B, right dp4; DPC 21296E, left dp4 or p4; DPC 21500K, right p4; DPC 22442H, left p4; DPC 21839B, left p4; DPC 23305D, right p4; DPC 21538C, left m1; DPC 21221C, left m1; DPC 21294C, left m1; DPC 21358C, right m1; DPC 21360B, right m1; DPC 21374B, right m2; DPC 21452C, right m2; DPC 21500L, right m2; DPC 21538D, right m2; DPC 21839C, right m2; DPC 22442I, right m2; DPC 21360C, right m2; DPC 21221D, right m2; DPC 21296G, left m2; DPC 21294D, left m2; DPC 21306D, left m1 or m2; DPC 21374C, right m3; DPC 23305E, right m3; DPC 21452D, left m3; DPC 21358D, left m3; DPC 21839E, left dP4; DPC 21538E, left dP4; CGM 08-328A, right dP4; DPC 21220D, right dP4; DPC 21360E, right dP4; DPC 21294E, right P4; DPC 21371I, left P4; DPC 21488D, left P4; DPC 21452E, right M1 or M2; DPC 21347D, right M1 or M2; DPC 21747I, right M1 or M2; DPC 22442J, right M1 or M2; DPC 21220E, right M1 or M2; DPC 21358E, right M1 or M2; DPC 21458E, right M1 or M2; DPC 21374E, left M1 or M2; DPC 21371J, left M1 or M2; DPC 21293N, left M1 or M2; DPC 21294F, left M1 or M2; DPC 21358H, left M1 or M2; DPC 21360F, left M1 or M2; DPC 21488F, left M1 or M2;

DPC 21839F, left M1 or M2; DPC 23305F, left M1 or M2; DPC 21502C, left M1 or M2; DPC 21538F, left M1 or M2; DPC 21221E, left M1 or M2; DPC 21296H, left M1 or M2; DPC 21452F, left M1 or M2; DPC 21500M, left M1 or M2; DPC 21293O, right M3; DPC 21221F, right M3; CGM 08-328B, left M3; DPC 21358G, left M3; DPC 21488G, left M3.

Type Locality—Birket Qarun Locality 2 (BQ-2).

Age—About 37 Ma, earliest Priabonian in age (earliest late Eocene).

Geographic Distribution—Northeastern end of Birket Qarun, west of Kom Aushim, Fayum Depression, Egypt (Figs. 1, 2).

Diagnosis—Differs from all other known anomaluroids in combining the following features: large size (molars much larger than those of all other Paleogene anomaluroids, see Fig. 5); relatively broad palate; upper molars bear a well-developed mure as an extension of a trenchant and mesiolabially oriented anterior arm of the hypocone; upper teeth relatively round in outline; upper molar mesostyle large and distinct; neo-endoloph massive but short on upper molars, leaving the lingual sinus broadly open; upper fourth premolars bear a large hypocone and a shallow ectoflexus. Differs from contemporaneous *Pondaungimys* from Myanmar (Dawson et al., 2003; Marivaux et al., 2005) and *Nementchamys* from Algeria (Jaeger et al., 1985) in lacking extensive enamel crenulation on the upper and lower teeth, and in having a relatively well-developed anterior arm of the entoconid on p4.

Description

Mandible—The mandible (Figs. 4A, 8) is robust and the horizontal ramus is relatively shallow. Available specimens preserve the dorsal part of the mandibular corpus and the first and second molars in place, but are missing the ascending ramus. The base of the coronoid process is anterior to the alveolus of the lower third molar, and obscures the m3 roots in lateral view. The diastema is shallow, and only extends down to about the same level as the alveoli of p4. The dorsal and ventral masseteric ridges, which delimit the masseteric fossa, meet anteriorly just below the posterior part of the first molar. The mental foramina are either single or double, and situated just below the middle of the diastema.

Lower Dentition—The complete lower dentition is known from isolated teeth (Fig. 6). The lower deciduous fourth premolar (Figs. 6A–J, 8B) is longer than it is wide. In some individuals, the tooth is particularly long relative to width, and there is some variation in dp4 size within the hypodigm. The tooth bears a pentalophodont occlusal pattern with a somewhat triangular outline due to a broad talonid and a narrow trigonid (the distal root is larger than the mesial root). The metaconid is crestiform and is either transverse to the small protoconid, or more anteriorly placed. The metaconid is connected to the protoconid via a strongly curved anterolophid that delimits the mesial border of a large anterior basin. In unworn specimens, the anteroconid is visible as a small cusp located on the mesial margin, but this cusp disappears with wear. The posterior arm of the protoconid is transversely oriented, and connects the protoconid and the metaconid, which together form the distal margin of the anterior basin of the tooth. The middle basin is open lingually due to the absence of the anterior arm of the entoconid and the posterior arm of the metaconid. In most specimens, the mesolophid runs lingually from the distal part of the ectolophid and divides the middle basin into two roughly equal fossae. The mesolophid terminates on a well-developed mesostylid. In a few specimens, the mesolophid is interrupted. A well-developed ectolophid attaches to the junction between the hypolophid and the anterior arm of the hypoconid. The crestiform hypoconid, which is oriented mesiolabially–distolingually, is placed transverse to the entoconid, and its anterior portion extends mesially within the sinusid. A well-developed posterolophid courses across the distal border of the crown, connects the hypoconid and the entoconid, and delimits the posterior basin of the tooth. There is no hypoconulid.

The lower fourth premolar (Fig. 6K–O) has a similar occlusal morphology to that of the dp4, but it is larger in size, is relatively short, and has a buccolingually broader outline. It also differs in having a robust and tall anterior arm of the entoconid that connects that cusp to the mesostylid, closing the lingual side of the posterior half of the middle basin. Some specimens bear a crest running longitudinally from a small protoconid within the anterior basin.

The m1 and m2 (Figs. 6P–E', 8D, F, G) are also pentalophodont but have three roots (two mesial and one distal). The m1 is semi-rectangular in outline and is relatively long when compared with the m2. The anterolophid runs labially from the metaconid to weakly fuse with the anterior side of the protoconid, delimiting the anterior portion of the crown. In some cases, the anterolophid is interrupted near its midpoint (Fig. 6R). Some specimens bear a very low and short crest that is placed mesial to the protoconid (Fig. 6B'), presumably representing the remnants of an anterocingulid. The metaconid is crestiform, placed transverse to the protoconid, and is sometimes split along its length by a shallow notch. The metaconids on the m1–2 are larger than those of p4, and contact a well-developed posterior arm of the protoconid (metalophulid II) that is either transversely or slightly anterolingually oriented. In some individuals, the metalophulid II is interrupted just before it reaches the metaconid (Fig. 6Q–R). The mesolophid runs lingually within the middle basin from near the junction of the ectolophid and the anterior arm of the hypoconid, and fuses with a well-developed mesostylid lingually. In most specimens, the anterior arm of the entoconid and posterior arm of the metaconid are absent, leaving the mesostylid isolated on the lingual wall of the tooth. In some cases (Fig. 6C'), the anterior arm of the entoconid is well developed and contacts the mesostylid. A well-developed hypolophid runs labially from the entoconid and reaches the anterior arm of the hypoconid near that crest's junction with the ectolophid. The entoconid is positioned opposite to the hypoconid. The posterolophid courses across the posterior wall of the tooth, and connects the hypoconid and the entoconid, delimiting the posterior basin of the tooth. The hypoconulid is absent. The labial sinusid is wide and deep.

The occlusal pattern on m3 is similar to that of m1 and m2, but differs in combining the following features: relatively small in size; the trigonid is slightly larger than the talonid; middle portion of the lingual margin is concave; mesostylid is relatively small; and the posterolophid is smoothly curved.

Maxilla—A left maxillary fragment of *K. qarunensis* bears alveoli of P4 and M1 (Fig. 4B). The infraorbital ridge of the maxilla is broad, indicating that *Kabirmys* was hystricomorphous; the infraorbital foramen was evidently relatively broad when compared with those of *Anomalurus* and *Pondaungimys*. On the ventral surface of the maxilla, there is a low ridge extending mesially from the alveolus of the lingual root of P4, roughly parallel to the intermaxillary suture, which defines a shallow fossa anterior to the tooth row. A similar ridge and fossa occur in *Anomalurus*, *Idiurus*, and *Pondaungimys*; the palate of *Pedetes* has an anteriorly oriented ridge near the base of P4 as in these taxa, but there is no ventrally facing fossa in *Pedetes*. The palate is fairly flat and broad throughout its length as in *Pondaungimys*, and it is not narrow or anteriorly concave as in *Anomalurus*, or narrow and elongate anterior to the toothrow, as in *Idiurus*. The anterior portion of the maxilla extends along the same plane as the posterior portion, and preserves part of the suture for the premaxilla. The lateral border of the incisive foramen is defined along the anterior and medial edge of the specimen. In dorsal view, the infraorbital fissure is absent and the base of the nasal fossa is broad. The zygomatic arch is thick and protrudes laterally at the level of P4, giving a broad ventral area for attachment of the superficial

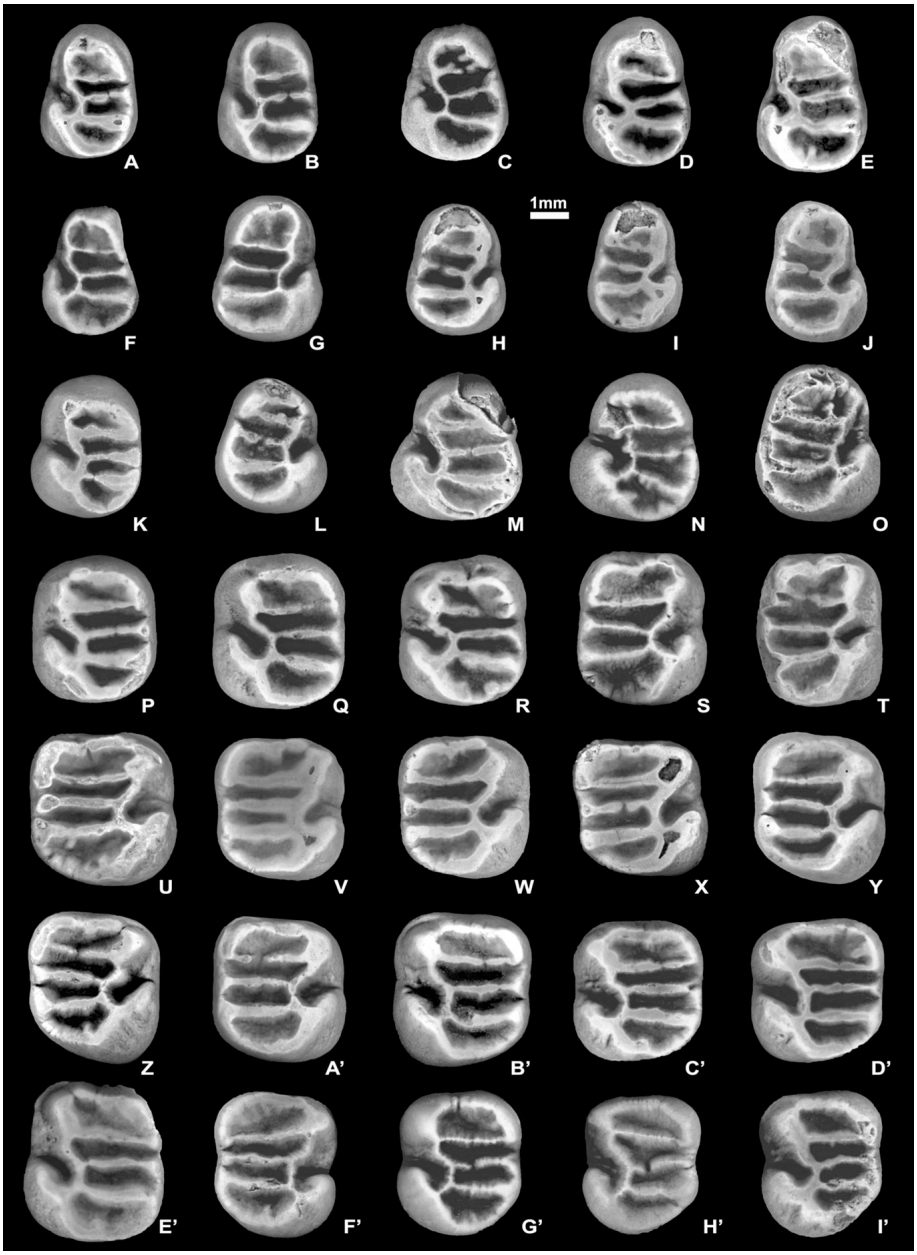

FIGURE 6. Isolated lower teeth of *Kabirmys qarunensis*, gen. et sp. nov. **A**, DPC 21374A, left dp4; **B**, DPC 21452B, left dp4; **C**, DPC 21221B, left dp4; **D**, DPC 21360A, left dp4; **E**, DPC 21839A, left dp4; **F**, DPC 23305C, left dp4; **G**, DPC 21294B, right dp4; **H**, DPC 21538B, right dp4; **I**, DPC 21293M, right dp4; **J**, DPC 21358B, right dp4; **K**, DPC 21296E, left dp4 or p4; **L**, DPC 21500K, right p4; **M**, DPC 22442H, left p4; **N**, DPC 21839B, left p4; **O**, DPC 23305D, right p4; **P**, DPC 21538C, left m1; **Q**, DPC 21221C, left m1; **R**, DPC 21294C, left m1; **S**, DPC 21358C, right m1; **T**, DPC 21360B, right m1; **U**, DPC 21374B, right m2; **V**, DPC 21452C, right m2; **W**, DPC 21500L, right m2; **X**, DPC 21538D, right m2; **Y**, DPC 21839C, right m2; **Z**, DPC 22442I, right m2; **A'**, DPC 21360C, right m2; **B'**, DPC 21221D, right m2; **C'**, DPC 21294D, left m2; **D'**, DPC 21296G, left m2; **E'**, DPC 21306D, left m1 or m2; **F'**, DPC 21374C, right m3; **G'**, DPC 23305E, right m3; **H'**, DPC 21452D, left m3; **I'**, DPC 21358D, left m3.

masseter muscle. Placement of the root of the jugal process of the maxilla opposite P4 is similar to the condition in *Anomalurus* and *Pondaungimys*, but differs from the much more anterior placement of the root in *Idiurus* and *Pedetes*.

Upper Dentition—The upper deciduous premolar (Fig. 7A–E) has a mesiodistally limited lingual margin, leading to a somewhat triangular outline. The tooth bears recognizable cusps that are integrated into a pentalophodont occlusal pattern. The anteroloph forms the anterior border of the tooth, and runs from the crestiform protocone to fuse to a well-developed parastyle that is as large as the paracone. The parastyle either joins the base of the paracone, or terminates in front of that cusp, leaving a shallow notch in the labial wall of the anterior basin. The paracone and protocone are joined by a well-developed and transversely oriented protoloph. A well-developed mesolophule divides the middle basin into two roughly equal parts, and runs labially from a trenchant anterior arm of the hypocone to merge with a distinct mesostyle. The mesolophule is sometimes interrupted near its midpoint (Fig. 7A, D). The mesostyle and the posterior arm of the paracone occupy most of the labial wall between the paracone and the metacone. In one specimen (DPC 21360E, Fig. 7D), the posterior arm of the paracone is interrupted by a shallow notch. There is no anterior arm of the metacone, leaving the labial wall of the middle basin open between the metacone and mesostyle. A well-developed mure also runs longitudinally within the middle basin as a mesial extension of the anterior arm of the hypocone, and forms a barrier between the anterior division of the middle basin and the lingual sinus. The neo-endoloph is low, connects the protocone and the hypocone, and delimits the lingual wall of the sinus. A well-developed metaloph connects the metacone and the anterior arm of the hypocone and has variable courses (either heading directly towards the anterior arm of the hypocone, or trending lingually and then turning mesially to join the anterior arm of the hypocone). The metaconule is absent. The

FIGURE 7. Isolated upper teeth of *Kabirmys qarunensis*, gen. et sp. nov. **A**, DPC 21839E, left dP4; **B**, DPC 21538E, left dP4; **C**, CGM 08-328A, right dP4; **D**, DPC 21220D, right dP4; **E**, DPC 21360E, right dP4; **F**, DPC 21294E, right P4; **G**, DPC 21371I, left P4; **H**, DPC 21488D, left P4; **I**, DPC 21452E, right M1 or M2; **J**, DPC 21347D, right M1 or M2; **K**, DPC 21747I, right M1 or M2; **L**, DPC 22442J, right M1 or M2; **M**, DPC 21220E, right M1 or M2; **N**, DPC 21358E, right M1 or M2; **O**, DPC 21458E, right M1 or M2; **P**, DPC 21374E, left M1 or M2; **Q**, DPC 21371J, left M1 or M2; **R**, DPC 21293N, left M1 or M2; **S**, DPC 21294F, left M1 or M2; **T**, DPC 21358H, left M1 or M2; **U**, DPC 21360F, left M1 or M2; **V**, DPC 21488F, left M1 or M2; **W**, DPC 21839F, left M1 or M2; **X**, DPC 23305F, left M1 or M2; **Y**, DPC 21502C, left M1 or M2; **Z**, DPC 21538F, left M1 or M2; **A'**, DPC 21221E, left M1 or M2; **B'**, DPC 21296H, left M1 or M2; **C'**, DPC 21452F, left M1 or M2; **D'**, DPC 21500M, left M1 or M2; **E'**, DPC 21293O, right M3; **F'**, DPC 21221F, right M3; **G'**, CGM 08-328B, left M3; **H'**, DPC 21358G, left M3; **I'**, DPC 21488G, left M3.

well-developed posteroloph courses around the posterior margin of the tooth, running labially from the hypocone to either weakly join the base of the metacone, or leaving a small notch posterolingual to that cusp. One specimen (CGM 08-328A, Fig. 7C) exhibits complex crenulation of the occlusal surface, whereas this feature is absent in other specimens.

The permanent premolar (P4, Fig. 7F–H) is as large as, or possibly even larger than, M1. P4 has the same basic occlusal pattern as that of dP4, but is larger, broader, and longer, and has a somewhat semi-quadrate outline. When compared with the dP4, the lingual portion of P4 is long, has a relatively large protocone and hypocone, and a narrow sinus that is open lingually because the protocone is oblique and pinched labiolingually. The anteroloph and protoloph are relatively short when compared to the posteroloph and metaloph. As on dP4, in some individuals the mesolophule is interrupted in the middle basin.

The M1 and M2 (Fig. 7I–D') are also pentalophodont and have an occlusal configuration similar to that of the dP4 and P4, but the molars have well-developed lophs and relatively robust cusps. It is difficult to identify these teeth to locus, and both are described together. The anterostyle varies between occasionally being very distinct (see, e.g., Fig. 7V, Y) and, more commonly, being completely merged into the protocone (forming a long mesiolabially–distolingually crestiform cusp). The posterior part of the protocone extends distally toward the hypocone, and sometimes contacts the mesial base of the hypocone, forming an almost continuous and trenchant neo-endoloph, but the lingual sinus is generally open via a narrow and deep crevice. Some individuals bear a short crest protruding from the mesial portion of the hypocone (within the distal part of the middle basin), or a short crest protruding lingually from the parastyle (in the anterior basin). The metacone in some specimens is lingually positioned

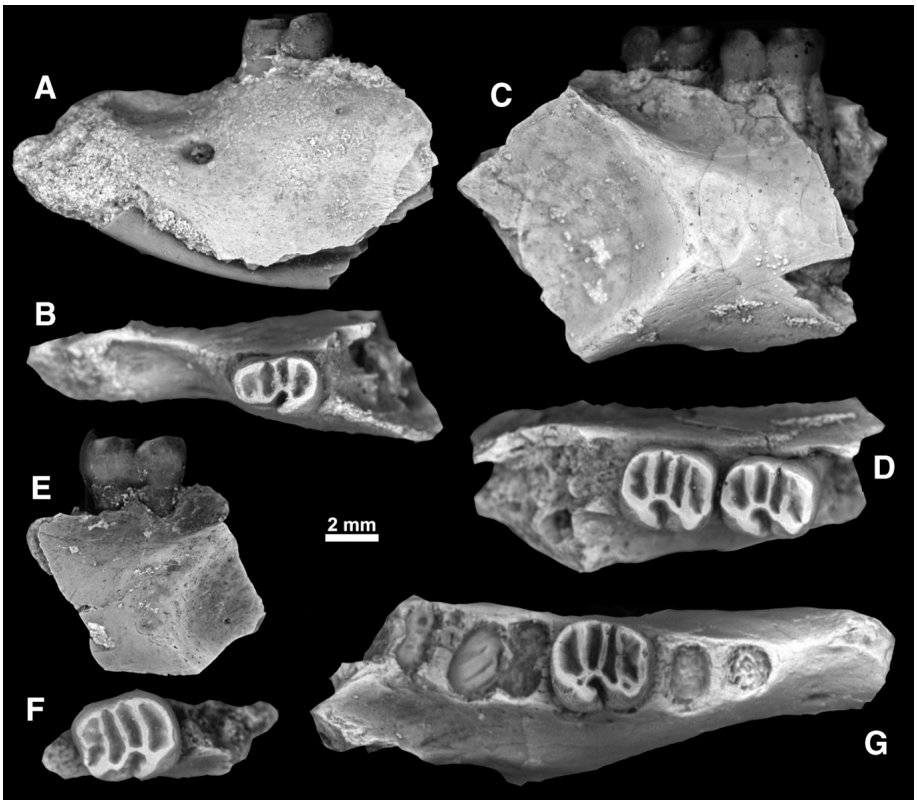

FIGURE 8. Mandibular fragments of *Kabirmys qarunensis*, gen. et sp. nov. **A–B,** CGM 08-289A, fragment of left mandible with dp4 and incisor in lateral (**A**) and occlusal (**B**) views; **C–D,** CGM 83698, holotype right mandible with m1–2 in lateral (**C**) and occlusal (**D**) views; **E–F**, CGM 21839G, left mandibular fragment with m1 in lateral (**E**) and occlusal (**F**) views; **G**, DPC 23305I, right mandible with m1 in occlusal view.

with respect to the paracone, leading to a more curved distolabial margin of the tooth. The metaloph has variable courses as in dP4.

The upper third molar is variable in size (Fig. 7E'–I'), is smaller than M1–2, and has a trapezoidal outline. The distal cusps, the metacone and hypocone, are reduced in size and are more lingually and labially positioned, respectively. A shallow ectoflexus occupies most of the labial wall and in some specimens, a crevice splits the mesostyle. Cusp placement on the posterior portion of the M3 crown is difficult to interpret. In most specimens, the posteroloph appears to be interrupted near the hypocone, and there is a crest running from the posteroloph to join with the hypocone or the anterior arm of the hypocone. This crest could be a remnant of the metaloph, which would imply that either the metacone was very close to hypocone, or the metaloph was derived from the posteroloph. One specimen (CGM 08-328B, Fig. 7G') differs from all others in having a very distinct metaloph that runs transversely across the posterior aspect of the tooth to contact the hypocone. This specimen also differs from other M3s in the hypodigm in having a relatively low posteroloph, a protoloph that is somewhat sinuous, an isolated mesostyle, and an anteroloph that is interrupted by crevices along its length.

COMPARISON AND REMARKS

Kabirmys is the largest known Eocene anomaluroid, and is markedly larger than the otherwise more derived contemporaneous and sympatric anomalurid *Shazurus* (Sallam et al., in press). The m1 area of *Kabirmys* is, on average, about 6 times that of *Shazurus*, and 2.5 times that of *Pondaungimys* and *Nementchamys* (Fig. 5). *Kabirmys* shares a number of dental and cranial features with other Eocene-to-Recent anomaluroids that were probably present in their last common ancestor—for instance, a large infraorbital foramen, a large permanent premolar, well-developed parastyles, anterostyles, mesostyles, anterolophs, and mesolophules on the upper molars, and strong mesostylids, well-developed ectolophids and mesolophids, complete posterolophids, and no hypoconulids on the lower molars. Furthermore, *Kabirmys* has a broad palate that is similar to those of Eocene *Pondaungimys* and Miocene *Paranomalurus bishopi*, and unlike extant *Anomalurus* and *Idiurus*, which have relatively narrow palates.

The occlusal configuration on the p4 of *Kabirmys* is similar to that of *Shazurus*, *Nementchamys*, and *Pondaungimys*, but *Kabirmys* has a relatively well-developed anterior arm of the entoconid. *Kabirmys* also lacks the well-developed posterior arm of the metaconid that fuses to the mesostylid in *Shazurus* and *Pondaungimys*. The p4 of *Kabirmys* is relatively short and wide when compared with that of *Pondaungimys*, lacks the mesoconid and hypoconulid, and further differs from that genus in having a posterior arm of the protoconid that is transversely oriented and roughly parallel to the mesolophid, rather than being obliquely oriented. The p4 of *Nementchamys* differs from that of *Kabirmys* and other Eocene anomaluroids in having a distinct mesostylid and mesolophid accessories. The lower premolars of the early Miocene anomalurids *Paranomalurus bishopi* and *Paranomalurus walkeri* are relatively long when compared with that of *Kabirmys*, have protoconids that are posteriorly placed with respect to the metaconid, and lack well-developed anterior arms of the entoconid.

The lower molars of *Kabirmys* differ from those of the Eocene zegdoumyids *Glibia* and *Zegdoumys* from the latest early, or earliest middle, Eocene of Algeria (Vianey-Liaud et al., 1994) in having a well-developed ectolophid, a robust mesostylid, a longer and more distinct mesolophid, and in lacking the mesoconid. Overall, the lower molars of *Kabirmys* are very similar to those of *Shazurus*, but there are some notable differences. In *Shazurus*, the anterolophid is not continuous with the protoconid, and thus the anterior basin is open labially, whereas in

Kabirmys the anterior basin is completely closed. The lower molars of *Shazurus* further differ from those of *Kabirmys* in having broad and short basins, a well-developed posterior arm of metaconid, and variable presence of the anterior arm of entoconid (leading to an isolated mesostylid). Some *Kabirmys* individuals have an interrupted mesolophid and anterolophid, whereas this condition has never been observed in *Shazurus*. The lower molars of *Kabirmys* differ from those of *Pondaungimys* and *Nementchamys* primarily in lacking extreme development of enamel crenulation; the latter taxa also have a relatively short anterior basin and a well-developed posterior arm of metaconid that fuses with the mesostylid. The posterior arm of the protoconid in *Pondaungimys* is more mesiolingually oriented than that of *Kabirmys* (which is either transversely or distolabially oriented), and in *Pondaungimys* the mesoconid is present whereas it is absent in *Kabirmys*. The lower dentition of *Kabirmys* also shows great overall similarity to that of extant *Anomalurus*, but the latter bears relatively high-crowned teeth with pointed labial cusps (protoconid and hypoconid), and a relatively wider and longer premolar. The differences between the lower molars of *Kabirmys* and *Paranomalurus* are the same as those discussed above in the premolars.

Anomaluroid dP4s are rare in the fossil record, and the only other documented example is that of *Pondaungimys*. The dP4 of *Pondaungimys* differs from that of *Kabirmys* in having relatively weak development of crests and cusps, a metacone that is small and mesiodistally compressed, no metaloph, an isolated mesostyle, a metaconule, and an anteroloph that does not connect to either the protocone or the paracone. The dP4 of extant *Anomalurus* (Wood, 1962) is similar to that of *Kabirmys* in having a pentalophodont occlusal surface, an enlargement in the labial portion of the posteroloph, and an interrupted mesolophule (the latter feature is seen on only one specimen of *Kabirmys*). But the neo-endoloph on the dP4 of *Anomalurus* is well developed, the mesolophule runs from the labiolingually oriented anterior arm of the hypocone, and the mure is absent; *Kabirmys* has a very low and poorly developed neo-endoloph, its mesolophule runs labially from the mesiolabially oriented anterior arm of the hypocone, and the latter crest extends mesially to reach the middle of the protoloph as a complete mure.

The P4s of extant *Anomalurus*, Miocene *Paranomalurus bishopi* and *walkeri*, and Eocene *Shazurus* and *Nementchamys* share several characters not seen in *Kabirmys*, such as a somewhat triangular outline, a well-developed neo-endoloph that connects the protocone and hypocone (and closes off the lingual sinus), weak development of the mure, a smoothly concave anteroloph, and no development of the ectoflexus. The P4 of *Kabirmys* further differs from that of *Shazurus* in having a metaloph that contacts a well-developed anterior arm of the hypocone, instead of being oriented backward to contact the posteroloph. *Paranomalurus soniae* and *Kabirmys* share features of the P4 such as absence of the neo-endoloph and a mesiolabially oriented anterior arm of the hypocone. *Kabirmys*' P4 occlusal pattern is somewhat similar to that of *Pondaungimys*, but the latter has a neo-endoloph and a small shallow sinus, a relatively poorly developed mesolophule and metaloph, no mure, and accessory enamel crenulations.

The M1–2 of *Kabirmys* differ from those of *Shazurus* in having a more rounded outline of the crown, and in lacking Y-shaped accessory crests, a transversely oriented posterior arm of the hypocone, and an accessory labial cusp. The M1–2 of *Pondaungimys* differ from those of *Kabirmys* in being somewhat rectangular in outline rather than having a more rounded margin, and in having a well-developed neo-endoloph closing the sinus lingually. The metacone and mesostyle of *Kabirmys* are relatively large when compared with those of *Pondaungimys*, and the metaloph fuses with the anterior arm of the hypocone in *Kabirmys*, whereas this crest is interrupted lingually in *Pondaungimys*. *Pondaungimys* has a few features that are not seen in *Kabirmys*, such as very reduced protoconule and metaconule cusps and accessory crests in the vicinity of the mesolophule. The M3 of *Pondaungimys* is the largest tooth of the upper dentition and has a heart-shaped outline, but in *Kabirmys* this molar is the smallest tooth of the upper dentition, and is more trapezoidal in outline. The hypocone of the M3 of *Kabirmys* is relatively large and more lingually placed when compared with that of *Pondaungimys*.

The upper molars of *Nementchamys* differ from those of *Pondaungimys* and *Kabirmys* in lacking a well-developed anterior arm of the hypocone, and in having the middle basin covered with numerous crenulations that obscure the configuration of the major crests on the occlusal surface. *Nementchamys* also has a crest running transversely from the parastyle that fuses with the anterostyle. The labial wall bears two cusps between the paracone and metacone, whereas in *Kabirmys* and *Pondaungimys*, the mesostyle is the only cusp occupying this area. The upper molars of *Nementchamys* further differ from those of *Kabirmys* in having a well-developed neo-endoloph.

The morphological differences between the M1–2 of *Kabirmys* and those of early Miocene *Paranomalurus* and extant *Anomalurus* are more obvious. The external crests that encircle the occlusal surface on the M1–2 of *P. walkeri*, *P. bishopi*, and *Anomalurus* form a somewhat square outline, whereas these crests form a more rounded outline in *Kabirmys*. The M1–2 occlusal surface of *Kabirmys* differs from those of *P. walkeri*, *P. bishopi*, and *Anomalurus* in having recognizable cusps and in lacking a complete neo-endoloph. The anterior arm of the hypocone in *Kabirmys* is mesiolabially oriented and is continuous as a complete mure, whereas it is continuous with the metaloph and forms a transverse crest in *P. walkeri*, *P. bishopi*, and *Anomalurus*. The labial wall of *Kabirmys*' M1–2 has a large and distinct mesostyle, but this cusp is submerged into the labial wall in *P. bishopi* and *Anomalurus*, and fuses to the posterior arm of the paracone in *P. walkeri*. The M3 of *P. bishopi* is the smallest of the upper teeth as in *Kabirmys*, but the M3 of the former has a relatively well-developed metaloph; the metaloph is only well developed on one specimen of *Kabirmys*. Although the upper molars of *Kabirmys* share some features with those of *P. soniae* (e.g., absence of a neo-endoloph, presence of a distinct mesostyle, and a mesiolabially oriented anterior arm of the hypocone), the latter differs in having the metaloph interrupted lingually, and in having relatively narrow notches dividing the labial cusps.

The upper molars of *Kabirmys* share characters with *Glibia* and *Zegdoumys* that are probably primitive within Anomaluroidea. The upper molars of these zegdoumyids have a well-developed anterior arm of the hypocone and lack the complete neo-endoloph, as in *Kabirmys*. Furthermore, the upper molars of *Glibia* bear a well-developed mesostyle that occupies the labial wall between the paracone and metacone, as in *Kabirmys*. The somewhat trapezoidal outline of *Kabirmys*' M3 is similar to that of *Zegdoumys*. Pickford et al. (2008) recently described the new species *Glibia namibiensis*, based on a single isolated upper molar from the Paleogene of Namibia. *G. namibiensis* differs from *Kabirmys* in lacking the anterostyle, parastyle, and mure, and in having a relatively low anteroloph, a more transversely oriented anterior arm of the hypocone, a relatively weak mesolophule, and a relatively restricted and shallow lingual sinus. However, the two taxa are similar in lacking a complete neo-endoloph, and in having very well-developed mesostyle, protoloph, and metaloph.

PHYLOGENETIC ANALYSIS

We investigated the phylogenetic position of *Kabirmys* by adding the new genus to the morphological character matrix of Sallam et al. (2010), which was modified from that of Marivaux et al. (2005). The matrix also samples *Shazurus*, a highly

derived anomaluroid genus from BQ-2 that was described by Sallam et al. (2010). The character set includes 97 dental features and two cranial features (see Appendix 1). As detailed by Sallam et al. (2010), the matrix of Marivaux et al. (2005) was modified by adding discrete intermediate character states for features that were polymorphic within terminal taxa (see Appendices 1, 2), and the species *P. bishopi*, *P. soniae*, and *P. walkeri* were scored separately. Ordered multistate characters were scaled so that state changes within each character could contribute a maximum of one step to tree length. Parsimony analysis was performed in PAUP* 4.0b10 (Swofford, 1998), with 1000 replicates, TBR branch-swapping, and random addition sequence. Statistical support for clades was estimated by bootstrap analysis in PAUP*, also across 1000 replicates.

Following parsimony analysis of morphological features in PAUP*, a chronobiogeographic character (hereafter 'CBG' character; see Rossie and Seiffert, 2006, for full details) was added to the character matrix in Mesquite v. 2.6 (Maddison and Maddison, 2009). Chronobiogeographic analysis (i.e., parsimony analysis of the morphological character matrix with the CBG character included) allows for a secondary test of the most parsimonious tree(s) recovered by parsimony analysis of morphological features alone (Fig. 9A). In particular, chronobiogeographic analysis allows for a more explicit test of phylogenetic hypotheses that imply multiple trans-oceanic dispersal events (given reconstructed palaeogeography), by assigning one or more steps to tree length for all of the trans-oceanic dispersal events that are implied by a given cladogram. The CBG character is composed of multiple 'time/place' states, and transitions between time/place states are constrained by a step matrix that assigns steps for implied changes from one time/place to another time/place by combining steps for accrued stratigraphic 'debt' (as in stratocladistics; see, e.g., Fox et al., 1999); i.e., the number of stratigraphic zones that a lineage is reconstructed as having passed though unsampled, leaving so-called 'ghost lineages') and biogeographic 'debt' (trans-oceanic dispersal events that are required to have occurred over the course of the interval delimited by the earlier and later time period). Trees that require time/place changes to have occurred when the landmasses in question were connected do not incur biogeographic debt, but they might incur stratigraphic debt. As in the analysis of Sallam et al. (2010), we conservatively assigned only a single step for each trans-oceanic dispersal event, and one step for high-latitude dispersals between Asia and North America (outside of the Ypresian [early Eocene], when biogeographic debt is considered '0' due to intense global warming; see, e.g., Zachos et al., 2003; Wing et al., 2005). A much more detailed treatment of the theory and methodology underlying chronobiogeographic analysis, as well as its justification, was provided by Rossie and Seiffert (2006). We sampled one taxon, *Glibia namibiensis*, whose age is poorly constrained and could not be confidently assigned to only one of the stratigraphic units represented in our CBG character. We therefore examined the sensitivity of different CBG scorings for *G. namibiensis* by running two different chronobiogeographic analyses, with *G. namibiensis* being scored as late Lutetian (i.e., later half of the middle middle Eocene) in one analysis (Fig. 9B) and Bartonian (late middle Eocene) in another (Fig. 9C). The heuristic search algorithm in Mesquite v. 2.6 was employed to search for the shortest trees implied by both the morphological character state distribution and the CBG character. Each matrix was analyzed 100 times, with taxon order randomized before each replicate.

Parsimony analysis of morphological data alone places *Kabirmys* deep within the family Anomaluridae as the sister taxon of *Nementchamys* and *Pondaungimys*, implying extensive ghost lineages for *Anomalurus* and *Idiurus* (Fig. 9A). There is, however, very little statistical support for relationships within Anomaluroidea, and even the monophyly of undoubted anomaluroids is not strongly supported (bootstrap value of 58). The interrelationships of zegdoumyids, cricetids, and anomaluroids are unresolved in the analysis. Chronobiogeographic analysis in Mesquite v. 2.6 places the oldest undoubted anomaluroid, *Pondaungimys*, as the sister group of a monophyletic clade of African

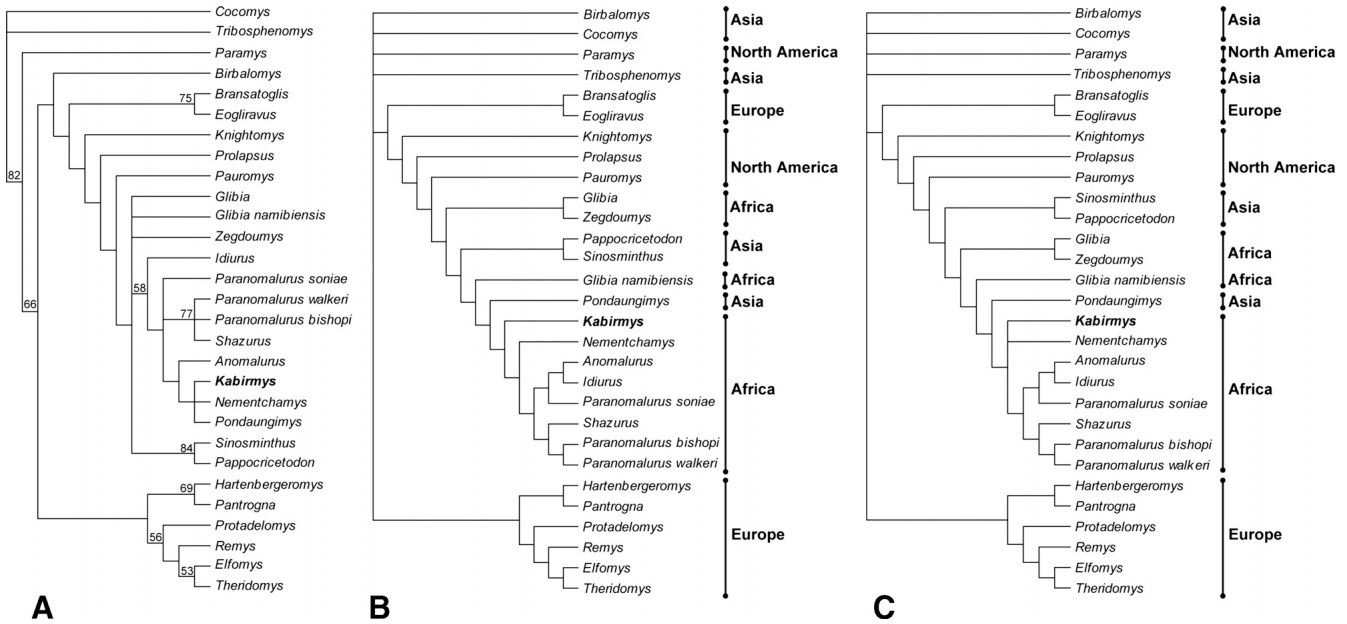

FIGURE 9. Most parsimonious trees calculated without (**A**) and with (**B**, **C**) the chronobiogeographic character. **A**, strict consensus of four most parsimonious trees recovered using the heuristic search algorithm in PAUP* 4.0b (tree length = 246.543, consistency index excluding uninformative characters = 0.3366, retention index = 0.6266, rescaled consistency index = 0.2143). Numbers above branches are bootstrap support values, based on 1000 pseudoreplicates. **B**, strict consensus of 18 trees of length 302.083334 recovered in Mesquite v. 2.6 following inclusion of the chronobiogeographic character, with '*Glibia*' *namibiensis* scored as late Lutetian in age. **C**, strict consensus of 22 trees of length 302.25 recovered in Mesquite v. 2.6 following inclusion of the chronobiogeographic character, with '*Glibia*' *namibiensis* scored as Bartonian in age.

anomaluroids that includes *Kabirmys* as one of its most basal members. Extant *Anomalurus* and *Idiurus* are placed as sister taxa in a clade with early Miocene *Paranomalurus soniae*. Assigning '*Glibia*' *namibiensis* to different stratigraphic intervals has a strong effect on tree topology. With '*G.*' *namibiensis* treated as late Lutetian (Fig. 9B), the species is placed as the sister taxon of all undoubted anomaluroids, but Cricetidae is placed as a sister taxon of this clade to the exclusion of Zegdoumyidae (Fig. 9B). However if '*G.*' *namibiensis* is assigned to the Bartonian interval, this species and the zegdoumyids *Glibia* and *Zegdoumys* are both placed as sister taxa of undoubted anomaluroids to the exclusion of Cricetidae. The latter topology clearly implies an African origin of Anomaluroidea from an ancestral group that would probably be identified as zegdoumyid. The intermediate placement of '*G.*' *namibiensis* in the two chronobiogeographic analyses suggests that there may be zegdoumyid-anomaluroid intermediates in the otherwise unsampled 10–15-Ma-long gap in the Lutetian and Bartonian of Afro-Arabia. Such a possibility is made all the more compelling by the presence of two anomaluroids at BQ-2 that are radically different in size and occlusal morphology, suggesting a much more ancient (Bartonian or Lutetian) common ancestor for these taxa in Africa.

DISCUSSION AND CONCLUSIONS

Overall, *Kabirmys*' dentition appears to be quite primitive, but interpretation of dental character polarities is complicated by the radically different placements of Eocene anomaluroids in our phylogenetic analyses (Fig. 9). For instance, the placement of *Kabirmys* in a clade with *Nementchamys* and *Pondaungimys* in the parsimony analysis of morphological features alone implies that some of *Kabirmys*' most distinctive features, such as the mure and weak neo-endoloph on the upper molars, are not characteristic of the anomaluroid morphotype and instead are simply autapomorphic within Anomaluridae. Given this topology, the weak p4 mesoconid that is seen in *Kabirmys*, *Nementchamys*, *Pondaungimys*, and the zegdoumyid *Zegdoumys* is reconstructed as an autapomorphy of *Zegdoumys*, and as a synapomorphy of a clade containing *Kabirmys*, *Nementchamys*, *Pondaungimys*, rather than as an ancestral feature of Anomaluroidea. When the CBG character is included, however, *Kabirmys*, *Nementchamys*, and *Pondaungimys* are placed as basal members of Anomaluroidea, and imply a very different ancestral morphotype for the clade containing known Eocene-to-Recent stem and crown anomalurids. For instance, the last common ancestor of *Pondaungimys* and later anomalurids is reconstructed as having had some crenulation of the molar enamel; weak posterior arm and anterior arm of the paracone and metacone, respectively; an incipient mure and a well-developed anterostyle on the upper molars; and a small mesoconid on p4 and the lower molar. The weak neo-endoloph of *Kabirmys* is nevertheless still reconstructed as an autapomorphy of that genus.

Kabirmys is, however, also the largest anomaluroid known from the Paleogene, being similar in size to some species of extant *Anomalurus* and Miocene *Paranomalurus*. It is particularly surprising to find that the two sympatric anomaluroids represented at Locality BQ-2, *Kabirmys* and *Shazurus*, are not only radically different in the occlusal morphology of their upper cheek teeth, but also differ markedly in body mass. This pattern is similar to that of living anomaluroids in west-central Africa, in which *Anomalurus* is much larger than tiny species of the genera *Idiurus* and *Zenkerella* (Kingdon, 1997; Dial, 2003). Might this be an indication that *Kabirmys* and *Shazurus* were partitioning their niches in a manner similar to modern sympatric anomaluroids? Unfortunately there is no way of determining whether *Kabirmys* or *Shazurus* were gliders based on available fossil material, but the occlusal morphology of *Kabirmys*' teeth is similar enough to that of like-sized *Anomalurus* that a broadly similar feeding adaptation seems likely. Kingdon (1997) observed that *Anomalurus* regularly feeds on the bark of a limited number of caesalpinioid and mimosoid species (e.g., miombo, awoura, ironwoods, owala oil trees, and velvet tamarinds), and hypothesized that anomalurid distribution is very closely tied to these trees. Molecular divergence estimates for caesalpinioid species indicate that the lineages on which *Anomalurus* depends arose much later in the Cenozoic (Lavin et al., 2005), but the initial diversification of the paraphyletic caesalpinioids likely took place early in the Eocene. If such a close relationship between anomaluroids and the distribution of certain tree species existed in the Eocene, this might provide an explanation for the disappearance of anomaluroids from northern African later in the Eocene, where the effects of global cooling through the later Paleogene, and most notably in the earliest Oligocene, might have removed suitable habitats from the region. At least four strepsirrhine primate lineages also disappeared from the Fayum area near the Eocene-Oligocene boundary (Seiffert, 2007), and, as with anomaluroids, these local extinctions might reflect changes in temperature and seasonality that affected forest structure in this part of northern Africa through the later Eocene and early Oligocene.

The major differences in morphology and body size between *Kabirmys* and *Shazurus* presumably also reflect an ancient divergence between these two taxa, most parsimoniously in Africa, given all of the topologies recovered in our analyses (Fig. 9). Together with *Nementchamys*, these taxa provide compelling evidence for an early morphological diversification of Anomaluroidea in Africa which must have been well underway by the late middle Eocene, and perhaps even earlier. By comparison, the hystricognathous rodents preserved at Locality BQ-2 (Sallam et al., 2009) show relatively little morphological diversity, hinting at a more recent dispersal of that group into Afro-Arabia, probably from Asia (e.g., Marivaux et al., 2002). The new evidence for an ancient evolutionary history of anomaluroids in Africa again raises the issue of whether the clade might be closely related to the enigmatic early or early middle Eocene Zegdoumyidae, which is, at present, the only rodent family known from this time period in Africa (Vianey-Liaud et al., 1994; Pickford et al., 2008). A related issue that has received less attention is the origin of the rodent family Pedetidae, another endemic African family that has now been quite confidently placed as the sister taxon of Anomaluridae based on molecular (e.g., Huchon et al., 2007; Montgelard et al., 2008; Blanga-Kanfi et al., 2009) and morphological (Tullberg, 1899; Bugge, 1974, 1985; Meng, 1990; Ruf et al., 2009) data. At present, the first record of Pedetidae is in the early Miocene of east Africa, and by this time the group's members had already evolved the extremely specialized, essentially bilophodont, crown morphology that is seen in extant *Pedetes* (MacInnes, 1957). Huchon et al. (2007) estimated that pedetids diverged from anomalurids at 56.8 Ma (95% confidence interval of 48.9–64.7 Ma), and Montgelard et al. (2008) recently provided even older estimates for the anomalurid-pedetid split. If this divergence occurred in Africa (as would be expected from available phylogenetic, fossil, and biogeographic data), the common ancestor of Anomaluridae and Pedetidae might trace back to a zegdoumyid-like form from the early Eocene of Afro-Arabia.

ACKNOWLEDGMENTS

This research was funded by U.S. National Science Foundation grant BCS-0416164 to E.L.S. and E.R.S. and BCS-0819186 to E.R.S. Funding was also provided by grants from The Leakey Foundation to E.R.S. Prithijit Chatrath (Division of Fossil Primates, Duke Lemur Center) managed fieldwork in Egypt. We are grateful to Dr. Hussein Hamouda (Egyptian Mineral Resources Authority) and the staff of EMRA and the Egyptian Geological Museum for supporting and facilitating our fieldwork in Egypt. Laurent Marivaux (I.S.E.M., Université Montpellier II)

kindly provided helpful comments on an earlier version of the manuscript, and casts and photographs of Eocene anomaluroids from Algeria and southeast Asia. M. Shahin assisted with phylogenetic analyses. J. Groenke and V. Heisey (Stony Brook University) assisted with preparation, molding, and casting. H.M.S.' research has been funded by the Egyptian Government and a Baldwin Fellowship from The Leakey Foundation. This is DLC publication #1184.

LITERATURE CITED

Barrow, E., E. R. Seiffert, and E. L. Simons. 2010. A primitive hyracoid (Mammalia, Paenungulata) from the early Priabonian (late Eocene) of Egypt. Journal of Systematic Palaeontology 8:213–244.

Blanga-Kanfi, S., H. Miranda, O. Penn, T. Pupko, R. DeBry, and D. Huchon. 2009. Rodent phylogeny revised: analysis of six nuclear genes from all major rodent clades. BMC Evolutionary Biology 9:71.

Bowdich, T. E. 1821. An Analysis of the Natural Classifications of Mammalia for the Use of Students and Travellers. J. Smith, Paris:115 pp.

Bugge, J. 1974. The cephalic arterial system in insectivores, primates, rodents and lagomorphs, with special reference to the systematic classification. Acta Anatomica 87(Suppl. 62):1–160.

Bugge, J. 1985. Systematic value of the carotid arterial pattern in rodents; pp. 355–379 in W. P. Luckett and J.-L. Hartenberger (eds.), Evolutionary Relationships among Rodents—A Multidisciplinary Analysis. Plenum Press, New York.

Cote, S., L. Werdelin, E. R. Seiffert, and J. C. Barry. 2007. Additional material of the early Miocene mammal *Kelba* and its relationship to the order Ptolemaiida. Proceedings of the National Academy of Sciences of the United States of America 104:5510–5515.

Dawson, M. R., T. Tsubamoto, M. Takai, N. Egi, S. T. Tun, and C. Sein. 2003. Rodents of the family Anomaluridae (Mammalia) from Southeast Asia (middle Eocene, Pondaung Formation, Myanmar). Annals of the Carnegie Museum 72:203–213.

Dial, R. 2003. Energetic savings and the body size distributions of gliding mammals. Evolutionary Ecology Research 5:1151–1162.

Fox, D. L., D. C. Fisher, and L. R. Leighton. 1999. Reconstructing phylogeny with and without temporal data. Science 284:1816–1819.

Gervais, F. L. P. 1849. Rongeurs; pp. 198–204 in M. C. d'Orbigny (ed.), Dictionnaire Universel d'Histoire Naturelle. M. M. Renard, Martinet et Cie, Paris.

Gill, T. 1872. Arrangement of the families of mammals with analytical tables. Smithsonian Miscellaneous Collections 230:1–98.

Gingerich, P. D. 1992. Marine mammals (Cetacea and Sirenia) from the Eocene of Gebel Mokattam and Fayum, Egypt: stratigraphy, age, and paleoenvironments. University of Michigan Papers on Paleontology 30:1–84.

Gunnell, G. F., E. L. Simons, and E. R. Seiffert. 2008. New bats (Mammalia: Chiroptera) from the late Eocene and early Oligocene, Fayum Depression, Egypt. Journal of Vertebrate Paleontology 28:1–11.

Huchon, D., P. Chevret, U. Jordan, C. W. Kilpatrick, V. Ranwez, P. D. Jenkins, J. Brosius, and J. Schmitz. 2007. Multiple molecular evidences for a living mammalian fossil. Proceedings of the National Academy of Sciences of the United States of America 104:7495–7499.

Jaeger, J.-J., C. Denys, and B. Coiffait. 1985. New Phiomorpha and Anomaluridae from the late Eocene of north-west Africa: phylogenetic implications; pp. 567–588 in W. P. Luckett and J.-L. Hartenberger (eds.), Evolutionary Relationships among Rodents—A Multidisciplinary Analysis. Plenum Press, New York.

Kingdon, J. 1997. The Kingdon Field Guide to African Mammals. Academic Press, San Diego, 465 pp.

Lavin, M., P. S. Herendeen, and M. F. Wojciechowski. 2005. Evolutionary rates analysis of Leguminosae implicates a rapid diversification of lineages during the Tertiary. Systematic Biology 54: 575–594.

Lavocat, R. 1973. Les rongeurs du Miocene d'Afrique Orientale I. Miocene inferieur. Memoires et Travaux de l'Institut de Montpellier 1:1–284.

Linnaeus, C. 1758. Systema naturae per regna tria naturae, secundum classes, ordines, genera, speciescum characteribus, differentiis, synomymis, locis, Editio decima reformata. Regnum animale. Editio decimal, reformata. Laurentii Salvii, Stockholm 1:824.

Liu, A., E. R. Seiffert, and E. L. Simons. 2008. Stable isotope evidence for an amphibious phase in early proboscidean evolution. Proceedings of the National Academy of Sciences of the United States of America 105:5786–5791.

MacInnes, D. G. 1957. A new Miocene rodent from east Africa. Fossil Mammals of Africa 12:1–35.

Maddison, W. P., and D. R. Maddison. 2009. Mesquite: A Modular System for Evolutionary Analysis. Version 2.6. Available at http://www.mesquiteproject.org

Marivaux, L., M. Vianey-Liaud, J.-L. Welcomme, and J.-J. Jaeger. 2002. The role of Asia in the origin and diversification of hystricognathous rodents. Zoologica Scripta 31:225–239.

Marivaux, L., S. Ducrocq, J. J. Jaeger, B. Marandat, J. Sudre, Y. Chaimanee, S. T. Tun, W. Htoon, and A. N. Soe. 2005. New remains of *Pondaungimys anomaluropsis* (Rodentia, Anomaluroidea) from the latest middle Eocene Pondaung Formation of Central Myanmar. Journal of Vertebrate Paleontology 25:214–227.

Meng, J. 1990. The auditory region of *Reithroparamys delicatissimus* (Mammalia, Rodentia) and its systematic implications. American Museum Novitates 2972:1–35.

Montgelard, C., E. Forty, V. Arnal, and C. Matthee. 2008. Suprafamilial relationships among Rodentia and the phylogenetic effect of removing fast-evolving nucleotides in mitochondrial, exon and intron fragments. BMC Evolutionary Biology 8:321.

Pickford, M., B. Senut, J. Morales, P. Mein, and I. M. Sanchez. 2008. Mammalia from the Lutetian of Namibia. Memoir, Geological Survey of Namibia 20:465–514.

Rossie, J. B., and E. R. Seiffert. 2006. Continental paleobiogeography as phylogenetic evidence; pp. 461–514 in J. G. Fleagle and S. Lehman (eds.), Primate Biogeography. Plenum, New York.

Ruf, I., S. Frahnert, and W. Maier. 2009. The chorda tympani and its significance for rodent phylogeny. Mammalian Biology 74:100–113.

Sallam, H. M., E. R. Seiffert, and E. L. Simons. 2010. A highly derived anomalurid rodent (Mammalia) from the earliest late Eocene of Egypt. Palaeontology 53:803–813.

Sallam, H. M., E. R. Seiffert, M. E. Steiper, and E. L. Simons. 2009. Fossil and molecular evidence constrain scenarios for the early evolutionary and biogeographic history of hystricognathous rodents. Proceedings of the National Academy of Sciences of the United States of America 106:16722–16727.

Seiffert, E. R. 2006. Revised age estimates for the later Paleogene mammal faunas of Egypt and Oman. Proceedings of the National Academy of Sciences of the United States of America 103:5000–5005.

Seiffert, E. R. 2007. Evolution and extinction of Afro-Arabian primates near the Eocene-Oligocene boundary. Folia Primatologica 78:314–327.

Seiffert, E. R., E. L. Simons, and Y. Attia. 2003. Fossil evidence for an ancient divergence of lorises and galagos. Nature 422:421–424.

Seiffert, E. R., T. M. Bown, W. C. Clyde, and E. L. Simons. 2008. Geology, paleoenvironment, and age of Birket Qarun Locality 2 (BQ-2), Fayum Depression, Egypt; pp. 71–86 in J. G. Fleagle and C. C. Gilbert (eds.), Elwyn Simons: A Search for Origins. Springer, New York.

Seiffert, E. R., J. G. M. Perry, E. L. Simons, and D. M. Boyer. 2009. Convergent evolution of anthropoid-like adaptations in Eocene adapiform primates. Nature 461:1118–1121.

Seiffert, E. R., E. L. Simons, W. C. Clyde, J. B. Rossie, Y. Attia, T. M. Bown, P. Chatrath, and M. Mathison. 2005. Basal anthropoids from Egypt and the antiquity of Africa's higher primate radiation. Science 310:300–304.

Swofford, D. L. 1998. PAUP*: Phylogenetic Analysis Using Parsimony (*and Other Methods), Version 4. Sinauer Associates, Sunderland, Massachusetts.

Thomas, H., J. Roger, S. Sen, M. Pickford, E. Gheerbrant, Z. Al-Sulaimani, and S. Al-Busaidi. 1999. Oligocene and Miocene terrestrial vertebrates in the southern Arabian peninsula (Sultanate of Oman) and their geodynamic and palaeogeographic settings; pp. 430–442 in P. J. Whybrow and A. Hill (eds.), Fossil Vertebrates of Arabia. Yale University Press, New Haven, Connecticut.

Tullberg, T. 1899. Über das System der Nagethiere: Eine Phylogenetische Studie. Nova Acta Regiae Societatis Scientiarum Upsaliensis 3:1–514.

Vianey-Liaud, M., and J.-J. Jaeger. 1996. A new hypothesis for the origin of African Anomaluridae and Graphiuridae (Rodentia). Palaeovertebrata 25:349–358.

Vianey-Liaud, M., J.-J. Jaeger, J.-L. Hartenberger, and M. Mahboubi. 1994. Les rongeurs de l'Eocène d'Afrique nord-occidentale [Glib Zegdou (Algérie) et Chambi (Tunisie)] et l'origine des Anomaluridae. Palaeovertebrata 23:93–118.

Wing, S. L., G. J. Harrington, F. A. Smith, J. I. Bloch, D. M. Boyer, and K. H. Freeman. 2005. Transient floral change and rapid global warming at the Paleocene-Eocene boundary. Science 310:993–996.

Winkler, A. J. 1992. Systematics and biogeography of Middle Miocene rodents from the Muruyur Beds, Baringo District, Kenya. Journal of Vertebrate Paleontology 12:236–249.

Wood, A. E. 1962. The juvenile tooth patterns of certain African rodents. Mammalology 43:310–322.

Zachos, J. C., M. W. Wara, S. Bohaty, M. L. Delaney, M. R. Petrizzo, A. Brill, T. J. Bralower, and I. Premoli-Silva. 2003. A transient rise in tropical sea surface temperature during the Paleocene-Eocene Thermal Maximum. Science 302:1551–1554.

Submitted June 22, 2009; accepted February 26, 2010.

APPENDIX 1. Modified character set of Marivaux et al. (2005) employed in phylogenetic analyses.

(1) Infraorbital foramen (maxilla): pseudo-myomorphous (0); sciuromorphous (1); protrogomorphous (2); hystricomorphous (3).
(2) Mandible: sciurognathous (0); hystricognathous (1).
(3) Hunter-Schreger bands (HSB): absent (0); present (1).
(4) Prisms per HSB: 1 (0); states 0 and 2 (1); 1–3 (2); states 2 and 4 (3); 2–4 (4).
(5) IPM crystallite arrangement in PI: sheath surrounding prisms (0); states 0 and 2 (1); parallel (2); states 2 and 4 (3); acute angular anastomosing (4).
(6) IPM thickness: thick (0); thin (1).
(7) Percentage of PE thickness: PE $\leq$ PI (0); PE reduced (<25%) (1).
(8) Band inclination relative to EDJ: 0 degrees (0); <10 degrees (1); 10–20 degrees (2).
(9) Size of P^4: $P^4 \geq M^1$ (0); $P^4 < M^1$ (1); minute (2); absent (3).
(10) Protoconule on P^4: inflated (0); weak (1); indistinct (2).
(11) Metaconule on P^4: strong (0); weak (1); indistinct (2).
(12) Protoloph on P^4: absent (0); incomplete (lingual protoloph absent) (1); complete (2).
(13) Metaloph on P^4: absent (0); states 0 and 2 (1); incomplete (lingual metaloph absent) (2); states 2 and 4 (3); complete (4); states 4 and 6 (5); submerged in posteroloph (6).
(14) Metacone on P^4: minute to absent (0); weak (1); strong (2).
(15) Hypocone: minute to absent (0); states 0 and 2 (1); weak (2); states 2 and 4 (3); strong (4).
(16) Mesostyle on P^4: absent (0); states 0 and 2 (1); weak and isolated (2); states 2 and 4 (3); strong (4).
(17) Anterocingulum on dP^4: weak (0); low and mesiodistally widened (1); high (2).
(18) Labial pericingulum on dP^4: present (0); states 0 and 2 (1); absent (2).
(19) dP^4 retention: P^4 replaces dP^4 (0); dP^4 retained (1).
(20) Talonid of P_4: narrow (0); $\leq$ trigonid (1); slightly wider than trigonid (2); greatly wider than trigonid (3).
(21) Predominant cuspids on P_4: strong metaconid (0); metaconid > protoconid (1); metaconid = protoconid (2).
(22) Hypolophid on P_4: absent (0); states 0 and 2 (1); present (2).
(23) Metaconid - protoconid compression on P_4: absent (0); states 0 and 2 (1); present (2).
(24) Metaconid/protoconid position on P_4: opposed (0); protoconid posterior (1).
(25) Hypoconulid on P_4: minute to absent (0); weak (1); strong (2).
(26) Mesoconid on P_4: absent (0); states 0 and 2 (1); weak (2).
(27) Ectolophid on P_4: absent (0); incomplete, anteriorly interrupted (1); complete, reaches protoconid from mesoconid (2).
(28) Metalophulid I on P_4: absent (0); incomplete, unconnected to metaconid (1); complete (2).
(29) Metalophulid II on P_4: absent (0); incomplete, unconnected to metaconid (1); complete (2).
(30) Anterior cingulid on P_4: absent (0); states 0 and 2 (1); low, lingually limited (2); states 2 and 4 (3); well developed (4).
(31) Posterior arm of metaconid (metastylar fold) on P_4: absent (0); weak and low (1); well developed and high (2).
(32) Size of P_4: $P_4 \geq M_1$ (0); $P_4 < M_1$ (1); minute (2); absent (3).
(33) Third upper premolar (P^3): present (0); reduced (1); absent (2).
(34) Third upper deciduous premolar (dP^3): present (0); reduced (1); absent (2).
(35) Anteroconid: absent (0); weak (1); large (2).
(36) Anterior cingulid: indistinct (0); low and weakly developed (1).
(37) Metaconid/protoconid position: opposed (0); protoconid posterior (1).
(38) Mesolophid: absent (0); states 0 and 2 (1); weakly developed (2); states 2 and 4 (3); reaches the lingual side (4).
(39) Posterior arm of metaconid (metastylar fold): absent (0); weak and low (1); well developed and high (2).
(40) Metalophulid I: absent (0); incomplete, medially interrupted (1).
(41) Metalophulid II: absent (0); incomplete, medially interrupted (1); complete (2).
(42) Talonid width: as wide as trigonid (0); slightly wider than trigonid (1); much wider than trigonid (2).
(43) Mesostylid: absent (0); weak (1); strong (2).
(44) Mesoconid: absent (0); weak (1).
(45) Hypoconulid: absent (0); weak (1).
(46) Ectolophid: absent (0); anteriorly interrupted (unconnected to protoconid) (1); complete (2).
(47) Hypocone: absent to minute (0); states 0 and 2 (1); weak (2); states 2 and 4 (3); strong (4).
(48) Hypocone position in relation to protocone: more lingual than the protocone (0); states 0 and 2 (1); same level as the protocone (2); states 2 and 4 (3); more labial (4).
(49) Mesostyle: absent (0); weak (1); strong (2).
(50) Parastyle: absent (0); small (1); well developed (2); forms an anterior lobe (on M^1) (3).
(51) Anterostyle: absent (0); weak (1); well developed (2).
(52) Anteroloph: absent (0); low and isolated from the protocone (1); high and connected to the protocone (2).
(53) Metaconule: strong, inflated (0); reduced (1); minute to indistinct (2).
(54) Metaconule position: on line between metacone and protocone (0); central cusp (1); submerged into the mure (2).
(55) Metaconule-hypocone connection: absent (0); present (1).
(56) Anterior arm of hypocone: absent (0); weakly developed (1); well developed (2).
(57) Mesolophule: absent (0); states 0 and 2 (1); incipient from metaconule (2); states 2 and 4 (3); reaches labial side (4).
(58) Protolophule II: absent (0); incipient (1); well developed (2).
(59) Protoconule: strong, inflated (0); reduced (1); submerged in the protoloph to absent (2).
(60) Anteroloph-protoloph connection (with a lingual anteroloph): absent (0); present (1).
(61) Metaloph connection: connected to metaconule (0); states 0 and 2 (1); connected on the anterior arm of hypocone (2); states 2 and 4 (3); turned posteriorly to join posteroloph (4).
(62) Metaconule-protocone connection (lingual metaloph): absent (0); states 0 and 2 (1); present (2).

(63) Endoloph: present (0); absent (1).
(64) Mure: absent (0); incipient (1); complete (2).
(65) Posterior outgrowth of protocone (neo-endoloph): absent (0); weak (1); forms a lingual wall (extends from the protocone to the hypocone) (2).
(66) Upper molars length/width proportions: length > width (0); length = width (1).
(67) Posterior arm of paracone: absent (0); weakly pronounced (1); high (connected to mesostyle) (2).
(68) Anterior arm of metacone: absent (0); weakly pronounced (1); high (connected to mesostyle) (2).
(69) Anterolophid (anterocingulid): absent (0); states 0 and 2 (1); incipient, low (2); states 2 and 4 (3); well developed (4).
(70) Anterolophulid: absent (0); present (1).
(71) Anteroconid: absent (0); incipient in anterolophid (1); well developed (2).
(72) Mesostylid: absent (0); states 0 and 2 (1); weak (2); states 2 and 4 (3); strong (4).
(73) Ectostylid: absent (0); present (1).
(74) Mesoconid: small to absent (0); simple cuspid (1); transversely elongate (2).
(75) Posterior arm of protoconid-mesoconid connection: absent (0); incomplete (1); present (2).
(76) Ectolophid: absent (0); states 0 and 2 (1); anteriorly incomplete (2); states 2 and 4 (3); complete, reaches protoconid (4).
(77) Mesolophid: absent (0); incipient (1); well developed, reaches the lingual side (2).
(78) Ectomesolophid: absent (0); states 0 and 2 (1); present (2).
(79) Protoconid/metaconid position: opposed (0); states 0 and 2 (1); protoconid posterior (2).
(80) Metaconid-protoconid height: protoconid < metaconid (0); protoconid = metaconid (1).
(81) Direction of the posterior arm of the protoconid: directed towards the metaconid (0); oblique, extending backwards (1).
(82) Paralophid-metaconid connection: absent (0); present (= metalophulid I) (1).
(83) Metalophulid I: complete (ancestral paralophid) (0); complex (antero-labial part of paralophid plus lingual part of protolophid) (1); weak to absent (2); remains of the antero-labial part of paralophid (lingual part of the paralophid or neo-formation) (3).
(84) Metalophulid II (protolophid = posterior arm of protoconid): well developed (0); states 0 and 2 (1); weak (2); states 2 and 4 (3); small to absent (4).
(85) Hypolophid: absent (0); states 0 and 2 (1); low, interrupted labially (2); states 2 and 4 (3); well developed (4).
(86) Anterior arm of hypoconid: absent (0); connects weakly to mesoconid (1); strong (2).
(87) Entoconid/hypoconid position: opposed (0); entoconid anterior (1).
(88) Hypoconulid: strong, inflated (0); states 0 and 2 (1); simple cuspid (2); states 2 and 4 (3); reduced, submerged into the posterolophid (4); states 4 and 6 (5); absent (6).
(89) Entoconid-hypoconid connection by posterolophid: present (0); states 0 and 2 (1); absent (2).
(90) Entoconid-hypoconid twinned on m3: absent (0); present (1).
(91) Trigonid height: higher than talonid (0); states 0 and 2 (1); as low as talonid (2).
(92) Trigonid width: narrower than talonid (0); as wide as talonid (1).
(93) Size of M_3 relative to M_2: $M_3 > M_2$ (0); states 0 and 2 (1); $M_3 = M_2$ (2); states 2 and 4 (3); $M_3 < M_2$ (4).
(94) Posterior arm of metaconid: absent (0); small (metastylid) (1); high metastylid (connected to mesostylid) (2).
(95) Anterior arm of entoconid: absent (0); small (1); high (connected to mesostylid) (2).
(96) Cuspids/crests: bunodont (0); states 0 and 2 (1); crests present but low (2); states 2 and 4 (3); lophodont (4).
(97) Cuspids: sharpened (0); inflated (1).
(98) Accesory enamel crestules on molars (wrinkles): absent (0); present (1).
(99) Chronobiogeographic character. For analysis with *Glibia namibiensis* scored as late Lutetian, character states are as follows: Late Paleocene of Asia (0); Ypresian of Asia (1); Ypresian of Europe (2); Ypresian of North America (3); early Lutetian of Europe (4); early Lutetian of Africa (5); late Lutetian of Africa (6); late Lutetian of Asia (7); late Lutetian of Europe (8); late Lutetian of North America (9); Bartonian of Asia (A); Bartonian of Europe (B); Priabonian of North America (C); Priabonian of Africa (D); Priabonian of Asia (E); Priabonian of Europe (F); Rupelian of Europe (G); Oligocene of Africa (H); Burdigalian of Africa (J); Recent of Africa (K). For analysis with *Glibia namibiensis* scored as Bartonian, character states are as follows: Late Paleocene of Asia (0); Ypresian of Asia (1); Ypresian of Europe (2); Ypresian of North America (3); early Lutetian of Europe (4); early Lutetian of Africa (5); late Lutetian of Asia (6); late Lutetian of Europe (7); late Lutetian of North America (8); Bartonian of Asia (9); Bartonian of Europe (A); Bartonian of Africa (B); Priabonian of North America (C); Priabonian of Africa (D); Priabonian of Asia (E); Priabonian of Europe (F); Rupelian of Europe (G); Oligocene of Africa (H); Burdigalian of Africa (J); Recent of Africa (K).

APPENDIX 2. Modified character-taxon matrix of Marivaux et al. (2005), with chronobiogeographic character added (character 99), and *Glibia namibiensis* scored as Bartonian. Missing and inapplicable data scored as '?.' Polymorphisms were scored as individual character states rather than as, e.g., '0/1' or '1/2.'

	1 10	20	30	40	50
Anomalurus	3010410202	224244???3	2202012024	212????????	??????4222
Birbalomys	3014000012	0242421102	2202112210	211?111020	2211124011
Bransatoglis	20???????12	2242222003	1020010012	21??111401	2111002211
Cocomys	2014000211	1000000001	2002000100	111????????	??????2011
Elfomys	3011000112	2242422203	1222110000	2122??????	??????4211
Eogliravus	?????????12	124222??03	1020021020	211?111220	2111002211
Glibia	?????????12	224242???0?	??????????	????110220	2211014221
Glibia namibiensis	??????????	??????????	??????????	??????????	??????4221
Hartenbergeromys	30???????11	0121030003	0220121000	211?000021	1211122211
Idiurus	30???????12	224242????3	2202000024	212????????	??????4212
Kabirmys	30??????02	2242441203	1200022024	01??101400	2120024322
Knightomys	2012000212	124220??03	1022120001	111???????	??????4212
Nementchamys	??12210011	225244??03	2202022024	1?????????	??????4222
Pantrogna	?011001011	1242120003	0020100010	21??000020	0111122111
Pappocricetodon	3010211103?	??????????	??????????	?322??????	??????4413
Paramys	2012001012	012222??03	1020121012	1122210010	1201112022
Paranomalurus bishopi	30???????12	224244???2	2204002024	1122??????	??????4220
Paranomalurus soniae	30???????12	224244???2	2202002024	012????????	??????4222
Paranomalurus walkeri	?0???????12	224244???2	2204002024	2122??????	??????4220
Pauromys	20???????11	1242401203	1012001112	222?110020	1111004211
Pondaungimys	3012210112	2222441203	1200122014	211????????	??????4222
Prolapsus	2012001111	122122??03	1022020012	1122??????	??????4221
Protadelomys	3014001012	1222241003	1222020000	2122001020	0111004221
Remys	3011010112	0222201203	1202220000	1122000021	0210104211
Shazurus	?????????12	224244????3	2204002024	21????????	??????4120
Sinosminthus	??????????	?????????0?	??????????	?322??????	??????4211
Theridomys	3012000212	226242??03	2212020000	2022101210	0110004211
Tribosphenomys	200?0012??	??????0000	2002?00210	011?010010	0201112001
Zegdoumys	??122100??	?????????03	1002021012	1?????????	??????4211

	60	70	80	90	99
Anomalurus	2422124020	2010414240	0400042002	0?20420600	21222400K
Birbalomys	1200000010	0200012010	0201030002	0102420120	210222001
Bransatoglis	122?000020	0200004140	0002002020	0?20200600	21?20400F
Cocomys	1200000000	0200010000	0001000002	0102000200	000000001
Elfomys	1411122020	4010010020	2000201002	1?14400600	21210200F
Eogliravus	1210000020	0200012040	1002001020	0?20010600	214202024
Glibia	1211122011	3011212240	1002001000	0?2040062?	21?102025
Glibia namibiensis	132??22020	2011312??	??????????	??????????	????????B
Hartenbergeromys	2400000011	0200012140	1101100000	1?14410500	212222022
Idiurus	2422120020	2010402140	0400002002	0?20410600	21420400K
Kabirmys	2422124020	2012313040	1400042?01	0?20420600	21303401D
Knightomys	1210110020	0010012040	0002001000	0?20200420	204102003
Nementchamys	2422124021	3011414240	1400042001	0?20420600	21?23402D
Pantrogna	2400000010	0200010040	1201101210	1?14210500	100200022
Pappocricetodon	1221122122	2011010041	1202021000	0?30410620	212202006
Paramys	0200000010	0200000040	1001000000	0?20000400	010100003
Paranomalurus bishopi	0422124020	2010414240	1400042002	0?20420600	21420400J
Paranomalurus soniae	1422124020	2010210040	2400042002	0?20420600	21420400J
Paranomalurus walkeri	0422124020	2010414040	1400042002	0?20420600	21420400J
Pauromys	1210113011	0010014040	1002001000	0?20200420	214202003
Pondaungimys	2422124010	2011412140	0401042002	0?20410600	200223029
Prolapsus	1220112010	0010010040	1002001000	0?20300420	212202008
Protadelomys	2400110000	2001010030	2000200020	1?14400200	210102027
Remys	1401112020	2000010000	0000200002	1?14400410	21200400A
Shazurus	0422124020	2010414240	1400042002	0?20420600	21?20400D
Sinosminthus	1222124221	2012010041	2201041122	0130410420	212202009
Theridomys	1411121020	4010010000	2200202022	1?14400620	21?22400F
Tribosphenomys	0200000010	0200000000	0001000000	0002010400	002000000
Zegdoumys	12??1220??	2010?14140	0201001000	0?2041062?	21?122025